

ELECTRONIC SUPPLEMENTARY INFORMATION

CO₂ capture enhancement for InOF-1: Confinement of 2-Propanol

Jonathan E. Sánchez-Bautista,^{†a} Bruno Landeros-Rivera,^{†b} Tamara Jurado-Vázquez,^a Ana Martínez,^{*,b,c}
Eduardo González-Zamora,^b Jorge Balmaseda,^c Rubicelia Vargas^{*,b} and Ilich A. Ibarra^{*,a}

^a *Laboratorio de Fisicoquímica y Reactividad de Superficies (LaFReS), Instituto de Investigaciones en Materiales, Universidad Nacional Autónoma de México, Circuito Exterior s/n, CU, Del. Coyoacán, 04510, Ciudad de México, Mexico.*

E-mail: argel@unam.mx

^b *Departamento de Química, Universidad Autónoma Metropolitana-Iztapalapa, San Rafael Atlixco 186, Co. Vicentina, Iztapalapa, C. P. 09340, Ciudad de México, México.*

^c *Instituto de Investigaciones en Materiales, Universidad Nacional Autónoma de México, Circuito Exterior s/n, CU, Del. Coyoacán, 04510, Ciudad de México, Mexico.*

1. Materials and measurements

All reagents and solvents were used as received from commercial suppliers without further purification. Powder X-ray diffraction (PXRD) data were collected under ambient conditions on a Bruker AXD D8 Advance diffractometer operated at 160 W (40 kV, 40 mA) for Cu K α_1 ($\lambda = 1.5406 \text{ \AA}$).

1.1 Sample preparation

Acetone-exchanged InOF-1: Samples of as-synthesized InOF-1 soaking in acetone, 10 times for 5 minutes.

Fully activated InOF-1: Acetone-exchanged samples of InOF-1 were activated at 453 K and a constant flow of N₂ (200 sccm) for 2 h.

***i*-PrOH@InOF-1:** Samples of acetone-exchanged InOF-1 were placed in a quartz sample holder inside a DVS Advantage 1 microbalance module, and activated at 453 K for 2 h. After that time, the samples were cooled down to room temperature (under a flow of N₂). Once activated, each sample was soaked in isopropanol vapour with the help of the previously mentioned device, selecting different values of partial pressure (2.26, 2.46, 2.68 and 2.76 % P/P_0) in order to achieve the desired weight percentages for this investigation (1.22, 2.05, 2.98 and 3.34 wt % of confined alcohol, respectively). The change in mass of the samples was monitored until the total mass reached a value consistent with the desired mass percentage of confined alcohol.

2. CO₂ adsorption experiments

Each of the *i*-PrOH@InOF-1 samples was loaded on a sample holder of the DVS Advantage 1 instrument. Once inside, a flow of CO₂ gas was allowed inside the sample chamber, in order to promote the capture of CO₂ inside the pores of the studied material until there was no variation of the mass of the sample. The obtained results, shown on Fig. S1, were plotted up to 13 minutes, when the CO₂ adsorption remained constant.

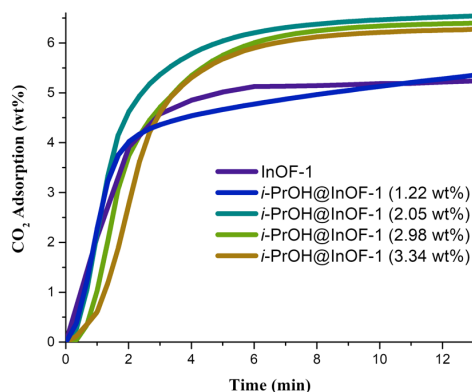


Fig. S1 Comparison of CO₂ uptake experiments performed at 303 K with a CO₂ flow of 120 sccm in InOF-1 (purple curve) and *i*-PrOH@InOF-1 at different weight percentages of confined isopropanol.

The error of CO₂ uptake amount considers two important factors: the critical temperature of the gas and the sensibility of the microbalance attached to the sorption instrument. Although the CO₂ capture was carried out near the critical temperature of CO₂, which introduces an error on the gas capture, the sensibility of the microbalance renders the first error factor as negligible, considering that said sensibility is of 0.1 μg. If an error during the CO₂ capture was present, the microbalance has the capacity to determine whether the registered mass uptake is still valid according to its sensibility and accuracy parameters. Thus, the approximate uptake CO₂ error is equal to 0.05 wt%.

3. Powder X-ray diffraction patterns of InOF-1

As stated on the main paper, PXRD pattern was collected after the synthesis of InOF-1. This was done in order to determine the phase purity of the synthesized MOF. The obtained pattern is compared with characteristic peaks that are located at 8.0, 9.2, 14.7, 16.3 and 18.7° (using a Cu lamp).¹

As seen on Fig. S2, the peaks with the highest intensity are present near 6 and 15°, which correspond with some of the characteristic peaks. Some other peaks with lower intensity, but that correlate with the characteristic peaks, are also present, confirming the phase purity of InOF-1. Additionally, the signals at 23, 25, 30 and 36° that appear on this experimental pattern can be found on the powder X-ray diffraction pattern reported by Chen *et al.* and on the simulated pattern of InOF-1,¹ thus confirming that the synthesized MOF is, indeed, InOF-1.

A second PXRD pattern was collected after the CO₂ capture experiments. This was done so as to determine the conservation of the crystallinity of InOF-1 after the cycles of adsorption of *i*-PrOH and CO₂, followed by desorption and activation of the samples.

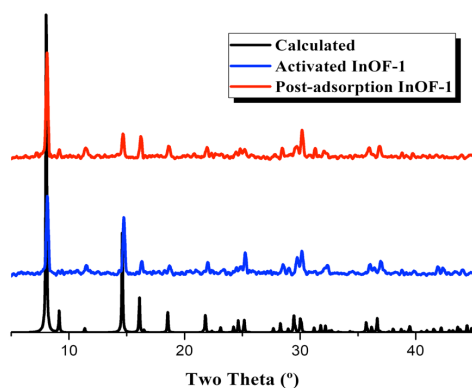


Fig. S2 Powder X-ray diffraction patterns of calculated (black), activated (blue) and post-adsorption (red) InOF-1.

Comparing the second pattern with the first one collected, the characteristic peaks are still present, albeit with lower intensity, save the one at 6°, which is more intense than in the first diffraction pattern. This

leads to the statement that the crystallinity of the sample of InOF-1 that was evaluated during the experimental procedure was retained. This is consistent with the behaviour observed by Sánchez-González *et al.*,² where the adsorption/desorption cycling for InOF-1 was studied, using DMF as the confined solvent.

4. Derivation of the isosteric enthalpy of adsorption for *i*-PrOH

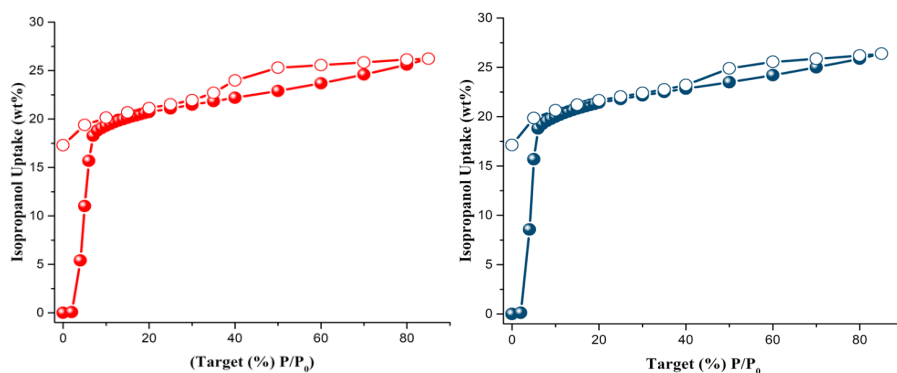


Fig. S3 *i*-PrOH adsorption isotherms at 293 K (red) and 303 K (blue) of InOF-1 from % $P/P_0 = 0$ to 85. Solid circles show adsorption phase. Open circles show desorption phase.

The isosteric enthalpy of adsorption was calculated with the help of isopropanol adsorption isotherms using the isosteric method, Q_{st} , by fitting a virial-type equation to both 293 and 303 K isopropanol adsorption isotherms.³ The virial-type equation that is used to fit both isotherms is the following one:⁴

$$\ln\left(\frac{n}{p}\right) = A_0 + A_1n + A_2n^2 \dots$$

where p is the pressure, n is the amount adsorbed and A_0 , A_1 etc. are virial coefficients. A_2 and higher terms can be ignored. A plot of $\ln(n/p)$ versus n should give a straight line at low surface coverage.³

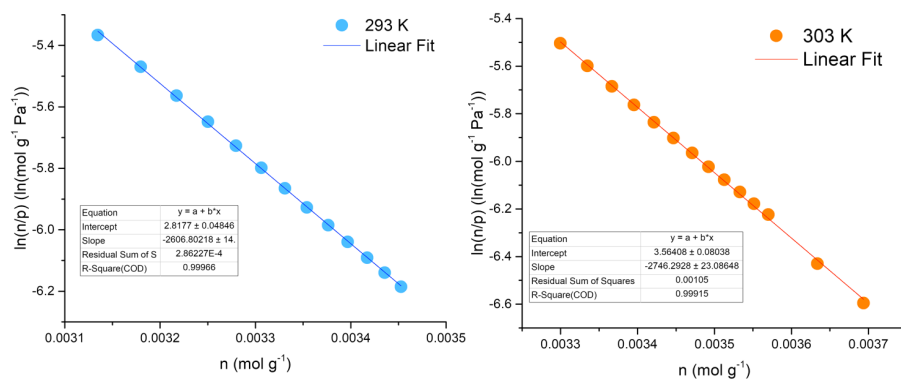


Fig. S4 Virial fitting plot for the adsorption of isopropanol on InOF-1 at 293 K (left) and 303 K (right).

Once obtained the plots, Q_{st} was calculated with the help of the Clausius-Clapeyron equation,⁴ obtaining a value of 55.151 kJ mol⁻¹:

$$Q_{st} = R \left(\frac{T_1 * T_2}{T_1 - T_2} \right) \ln \left(\frac{P_1}{P_2} \right)$$

5. Molecular calculations

Distances between donor (D) and acceptors (A) are given in angstroms; the electron density (ρ_{BCP}), laplacian (∇^2_{BCP}), positive definite energy density (G_{BCP}), virial (V_{BCP}) and electronic energy density (H_{BCP}) evaluated at the bond critical point are given in atomic units; the interaction energies (E_{int}), calculated via the Espinosa-Molins-Lecomte⁵ equation, are given in kcal mol⁻¹.

Table. S1 Geometrical and topological parameters of the interactions found in the coordination-molecular model.

	Type of contact	d(D...A)	Angle	ρ_{BCP}	∇^2_{BCP}	G_{BCP}	V_{BCP}	H_{BCP}	-G/V	E_{int}
Hydrogen bonds										
MOF-CO ₂	C-H...O	2.214	153.6	0.01291	0.06437	0.01293	-0.00977	0.00316	1.32	-3.1
MOF- <i>i</i> -OH	C-H...O	1.905	163.8	0.02859	0.13039	0.03065	-0.02871	0.00194	1.07	-9.0
MOF- <i>i</i> -OH	O-H...O	1.960	173.9	0.02590	0.09109	0.02242	-0.02206	0.00036	1.02	-6.9
<i>i</i> -OH-CO ₂	O-H...O	1.900	161.0	0.02350	0.10984	0.02525	-0.02304	0.00221	1.10	-7.2
Non-hydrogen bonds										
MOF-CO ₂	O...O	2.340	-	0.02408	0.15639	0.03192	-0.02475	0.00717	1.29	-7.8
MOF-CO ₂	O...O	3.212	-	0.00445	0.01740	0.00345	-0.00255	0.00090	1.35	-0.8

6. Periodical calculations

The atomic positions and cell parameters were taken from the Supporting Information provided by Peralta *et al.*⁶ The oxygen and hydrogen atoms of the μ -OH functional group show disorder and, therefore, two positions were reported. An average of both coordinates of each atom was taken as input. The energy convergence with regards to the number of k points was tested. The calculations were performed using a $2 \times 2 \times 2$ Monkhorst-Pack k-point mesh. Empirical dispersion was computed by a modified version of Grimme's scheme⁷ that parametrized for molecular crystals⁸.

References

1. Y. Chen, J. Xiao, D. Lv, T. Huang, F. Xu, X. Sun, H. Xi, Q. Xia and Z. Li, *Chem. Eng. Sci.*, 2017, **158**, 539-544.
2. E. Sánchez-González, E. González-Zamora, D. Martínez-Otero, V. Jancik and I. A. Ibarra, *Inorg. Chem.*, 2017 **56**, 5863-5872.
3. I. A. Ibarra, S. Yang, X. Lin, A. J. Blake, P. J. Rizkallah, H. Nowell, D. R. Allan, N. R. Champness, P. Hubberstey and M. Schröder, *Chem. Commun.*, 2011, **47**, 8304.
4. M. P. Suh, H. J. Park, T. K. Prasad and D.-W. Lim, *Chem. Rev.*, 2012, **112**, 782.
5. E. Espinosa, E. Molins and C. Lecomte, *Chem. Phys. Lett.*, 1998, **285**, 170.
6. R. A. Peralta, A. Campos-Reales-Pineda, H. Pfeiffer, J. R. Álvarez, J. A. Zárate, J. Balmaseda, E. González-Zamora, A. Martínez, D. Martínez-Otero, V. Jancik and I. A. Ibarra, *Chem. Commun.*, 2016, **52**, 10273.
7. S. Grimme, J. Antony, S. Ehrlich and H. Krieg, *J. Chem. Phys.*, 2010, **132**, 154104.
8. B. Civalleri, C. Zicovich-Wilson, L. Valenzano and P. Ugliengo, *CrystEngComm*, 2008, **10**, 405.